Available online at www.sciencedirect.com

ScienceDirect

Journal of Hazardous Materials 154 (2008) 1033–1039

Journal of Hazardous Materials

www.elsevier.com/locate/jhazmat

Degradation of 4-chlorophenol in TiO_2, WO_3, SnO_2, TiO_2/WO_3 and TiO_2/SnO_2 systems

Cheng-Fang Lin [a], Chung-Hsin Wu [b,*], Zong-Nan Onn [a]

[a] Graduate Institute of Environmental Engineering, National Taiwan University, 71, Chou-Shan Road, Taipei, Taiwan
[b] Department of Environmental Engineering, Da-Yeh University, 112, Shan-Jiau Road, Da-Tsuen, Chang-Hua, Taiwan

Received 23 August 2007; received in revised form 19 October 2007; accepted 3 November 2007
Available online 13 November 2007

Abstract

The present study was undertaken to evaluate the degradation performance of 4-chlorophenol (4-CP) using TiO_2/WO_3 and TiO_2/SnO_2 systems. A BET surface area analyzer, UV–vis spectroscopy, scanning electron microscopy (SEM), X-ray diffraction (XRD) and electron spectroscopy for chemical analysis (ESCA) were employed to characterize the photocatalyst. The band edge wavelength increased to 475 nm and gap energy decreased to 2.61 eV in the TiO_2/WO_3 system as compare to the single TiO_2. Although the specific surfaces area of TiO_2/WO_3 decreases due to its larger size as compared to either TiO_2 or WO_3, the 4-CP degradation efficiency significantly increased as compared to single TiO_2 or WO_3 system at 435 nm wavelength. The TiO_2/WO_3 degradation of 4-CP at 369 nm was in fact inhibited. For TiO_2/SnO_2, the degradation efficiency also suffered at 369 nm, and only slightly increased compared to otherwise hardly 4-CP degraded in single TiO_2 or SnO_2 system. Since there is a significant accumulation of byproducts, the buildup of these intermediates on the catalyst surface may be responsible for their poor performance.

Keywords: TiO_2; SnO_2; WO_3; 4-Chlorophenol; Photocatalyst

1. Introduction

Among different advanced oxidation processes, photocatalytic processes using semiconductor materials such as TiO_2 have been demonstrated as effective means for organic degradation. The hydroxyl radical mediated reaction depends on the type and dosage of catalyst, type and concentration of pollutant, light intensity, and operating conditions such as temperature, pH and irradiation time. In order to have a practical application, the use of visible light source along with an enhanced degradation rate is essential. This can be achieved via the modification of semiconductors [1], addition of transition metals [2,3] and other element doping [4] as well as use of coupled semiconductors. Serpone et al. [5] initially proposed interparticle electron transfer theory in that light excites semiconductor with a smaller energy band gap to photosensitize another semiconductor with a higher electrical potential and larger band gap to enhance photocatalytic reaction. Since then, coupled semiconductors have been used intensively for organic degradation in both aqueous and gas phase, including TiO_2/CdS [6,7], TiO_2/SnO_2 [8–11], TiO_2/ZnO [12] and TiO_2/WO_3 [13,14]. In general, the coupled systems exhibit higher degradation rate as well as the increased extent of degradation. The studies for comparing the coupled semiconductors with either UV or visible light; however, are scarce.

Consequently, the present study was undertaken to investigate the capability of coupled semiconductor systems to degrade a model compound (4-chlorpphenol, 4-CP). Two coupled system were used (TiO_2/SnO_2 and TiO_2/WO_3) at wavelength 369 or 435 nm so that the efficiencies of these two light irradiations could be compared. The physical characters of the coupled system were quantified by different methods: BET for the specific surface area; X-ray defractor (XRD) for crystal structure; UV–vis spectroscopy for determining band edge; scanning electron microscope (SEM) for size estimate; and X-ray electron spectroscopy (XPS) for determining distribution of SnO_2 or WO_3 in TiO_2. For comparison, a single system of WO_3, TiO_2, or SnO_2 was used.

---

* Corresponding author. Fax: +886 5 5334958.
E-mail address: chunghsinwu@yahoo.com.tw (C.-H. Wu).

0304-3894/$ – see front matter © 2007 Elsevier B.V. All rights reserved.
doi:10.1016/j.jhazmat.2007.11.010

2. Materials and methods

2.1. Materials

TiO_2 (Degussa P-25), SnO_2 (99%, Ridel-de-Haen) and WO_3 (99.9%, Hanawa) were used as received without any pretreatment. The model compound 4-CP was purchased from Avocado Co. Other chemicals used were reagent grade and deionized water was used. The coupled TiO_2/SnO_2 was synthesized via citric acid complexing method, followed the procedures of Lin et al. [15]. Briefly, $TiCl_4$ (98%, Fluka) and $SnCl_4$ (99%, Ridel-de-Haen) was added into the aqueous HCl solution; addition of citric acid; sonification mixing for 15 min and aging for 24 h; removal of HCl and H_2O upon heating; calcined the resultant precipitate at 400 °C for 3 h.

The synthesis for TiO_2/WO_3 followed the incipient wetness procedures of Kwon et al. [13]. Since a 3% molar ratio of WO_3 was found to exert a maximum decomposition of 1,4-dichlorobenezene in an TiO_2/WO_3 system [13,16], the initial molar ratio of H_2WO_4 (98%) and TiO_2 of 3:97 was used in an 25% ammonium solution. The mixture was dried, calcined at a rate of 100 °C/h to 400 °C; and then held for 2 h at 400 °C.

2.2. Experiments

The hollow cylindrical photo reactor has an effective volume of 3 L. The lamp (Wisdoms Electric & Lighting Co.) at either 369 or 435 nm was placed inside the tube. The overall study consisted of 3 single catalysts and two coupled systems for degrading 4-CP. All experiments were performed with the same power consumption (50 W), catalyst dosage (1.2 g/L), the initial 4-CP concentration (0.2 mM; initial TOC = 17.2 mg/L), and temperature (25 °C). Three pHs (4, 7 and 10) were used at the wavelength either 369 or 435 nm. The pH of the solution was controlled by adding HNO_3 and NaOH via an automatic titrator. During the course of experiments, the reactor content was continuously mixed (300 rpm) and aerated; samples were periodically withdrawn, filtered (0.45 μm) and filtrate was subsequently analyzed for TOC, chloride and 4-CP.

Several experiments were initially conducted to determine the extent of potential volatilization (no light, no catalyst with aeration), photolysis (no catalyst with aeration at 369 or 435 nm light) and catalytic reaction (catalyst without light and without aeration) of 4-CP. The results indicated no appreciable degradation of 4-CP after 200 min under the above three blank conditions. Reproducibility study was evaluated for several tests and the results were within 5%.

2.3. Analysis

The specific surface area of each photocatalyst was determined via BET method (Micrometric TrtStar 3000). The absorption of catalysts over the entire spectrum (190–800 nm) was monitored in a UV–vis spectroscopy (GBC, Cintra 20) to determine semiconductor band gap energy. The model compound, 4-CP, was monitored in an HPLC (Millipore Waters 600E, 470) at the detector wavelength 254 nm. The flow rate for mobile phase ($CH_3CN:H_2O:CH_3COOH = 50:50:1$) was 1 mL/min. TOC was measured in an OI TOC analyzer (Model 1010); chloride in an ion chromatograph (Dionex DX-120) with an eluent solution of $NaHCO_3/Na_2CO_3$.

The SEM diagrams were obtained from LEO (1530); XRD patterns were obtained using a Philips diffractometer (X'pert Pro) at 45 kV and current 40 mA. The wavelength of Cu Kα radiation used was 1.541 Å with a scan range of 2θ between 20° and 80°. Electron spectroscopy for chemical analysis (ESCA) was performed at 1486 eV (VG Scientific, ESCALAB 250) to investigate surface composition.

Sodium salcylate, as a trapping agent for hydroxyl radicals, was used to determine the extent of their production [17]. The byproducts of 2, 3-dihydroxybenzoic acid, 2, 5-dihydroxybenzoic acid and catechol were monitored at UV wavelength 318, 306 and 275 nm, respectively. The sum of hydroxylated derivates indicates the relative hydroxyl radical concentration.

3. Results and discussion

3.1. Characterization of catalysts

The BET results indicate lower specific surface area for the coupled TiO_2 catalysts as compared to single TiO_2 (Table 1). From the absorbance data of the entire UV–vis wavelength of each catalyst (Fig. 1), the band edge wavelength for each catalyst could be determined and the resultant band gap energies calculated [21] as shown in Table 1. While the band edge of TiO_2/WO_3 increases to 475 nm compared to the single TiO_2 (390 nm) or WO_3 (450 nm), that of TiO_2/SnO_2 (380 nm) slightly decreases

Table 1
Characterization of catalysts used in the present study

Sample	Band edge wavelength (nm)	Band gap energy (eV)	Specific surface area (m^2/g)	Size (nm)	Atom (%)
TiO_2	390	3.18	54[a]	24[b]	–
SnO_2	335	3.70	4.8[a]	59[b]	–
WO_3	450	2.76	1.0	42[c]	–
TiO_2/SnO_2	380	3.27	12.4	150	Ti2p:Sn3d = 95:5
TiO_2/WO_3	475	2.61	37.1	300	Ti2p:W4f = 76:24

[a] From Ref. [18].
[b] From Ref. [19].
[c] From Ref. [20].

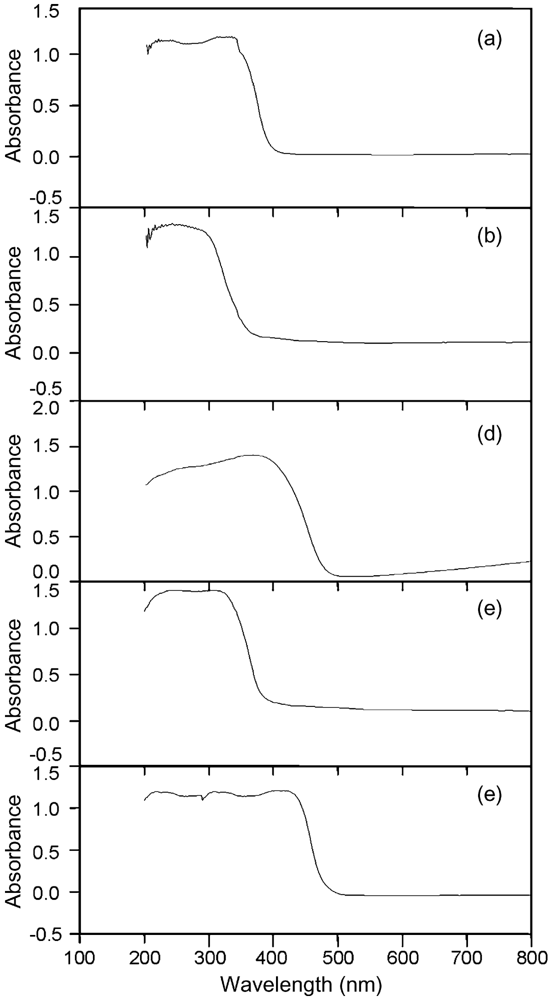

Fig. 1. The UV–vis spectrum of different catalyst (a) TiO_2, (b) SnO_2, (c) WO_3, (d) TiO_2/SnO_2, and (e) TiO_2/WO_3.

over the single TiO_2 (390 nm). In general, the results of band gap energy for WO_3 and TiO_2 are similar to those reported by others [14,22,23]; however, SnO_2 (3.7 eV) is higher than that (3.54 eV) of Sakthivel et al. [24].

Fig. 2 shows the SEM images of two coupled semiconductors. Both demonstrate almost uniform morphologies with the size TiO_2/SnO_2 about 150 nm and TiO_2/WO_3 about 300 nm. XRD analysis reveals that TiO_2 consists of mostly the anatase phase (Fig. 3a). The intensity of the coupled TiO_2/SnO_2 catalyst is almost the same as that of TiO_2 (Fig. 3a and c). However, there appears a separate phase of SnO_2 present in the coupled TiO_2/SnO_2 (Fig. 3b and c). This may be relevant to the subsequent performance since others have reported no SnO_2 structure could be detected in an TiO_2/SnO_2 system [25]. On the other hand, WO_3 may be incorporated into TiO_2 in the TiO_2/WO_3 system, since the diagrams for TiO_2 and TiO_2/WO_3 are exactly the same (Fig. 3a and e). The sharp peaks observed at $2\theta = 24.2°$, $34.2°$, $49.8°$ and $55.8°$ (Fig. 3d) were indicative of the monoclinic WO_3 [14]. It is noted that the initial molar ratio of TiO_2 to WO_3 was about 97:3, but the ESCA results (Table 1) indicate a much lower Ti:W ratio of 76:24.

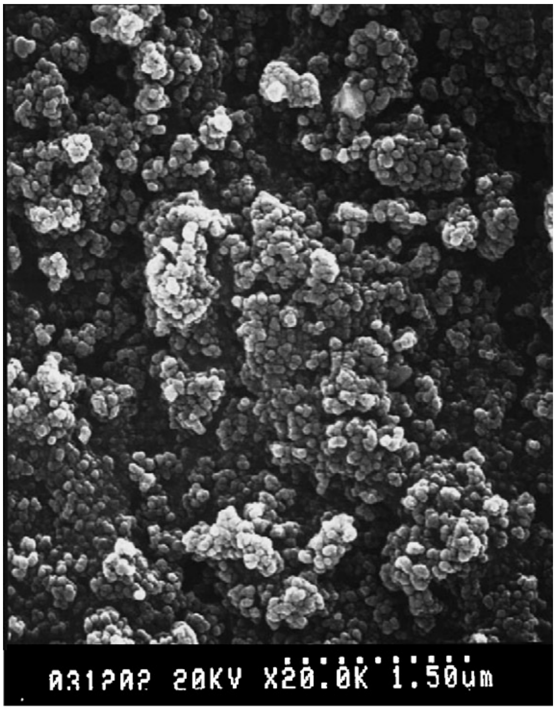

(a) TiO_2/SnO_2 (magnification: 20000)

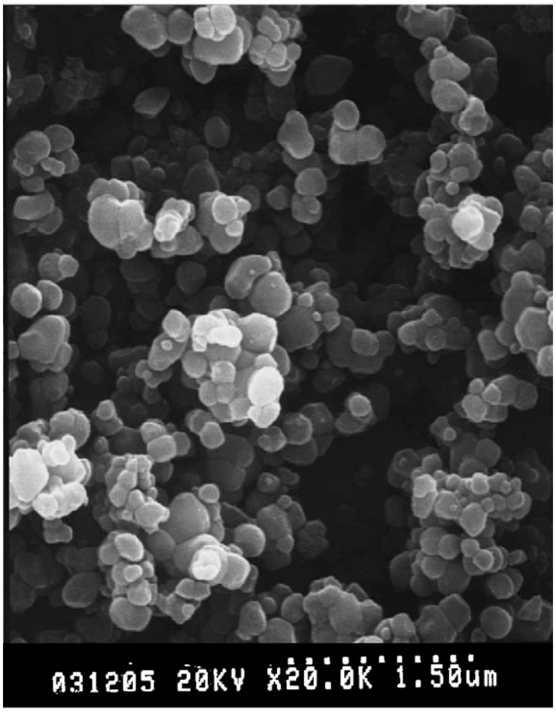

(b) TiO_2/WO_3 (magnification: 20000)

Fig. 2. SEM diagrams for coupled semiconductors (a) TiO_2/SnO_2 and (b) TiO_2/WO_3.

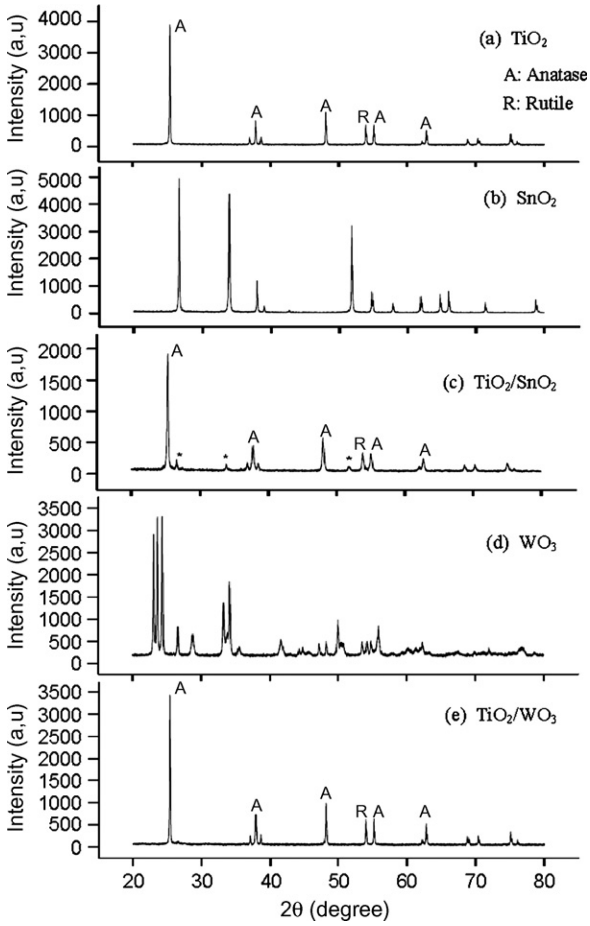

Fig. 3. XRD analysis of different semiconductors (a) TiO_2, (b) SnO_2, (c) TiO_2/SnO_2, (d) WO_3, and (e) TiO_2/WO_3.

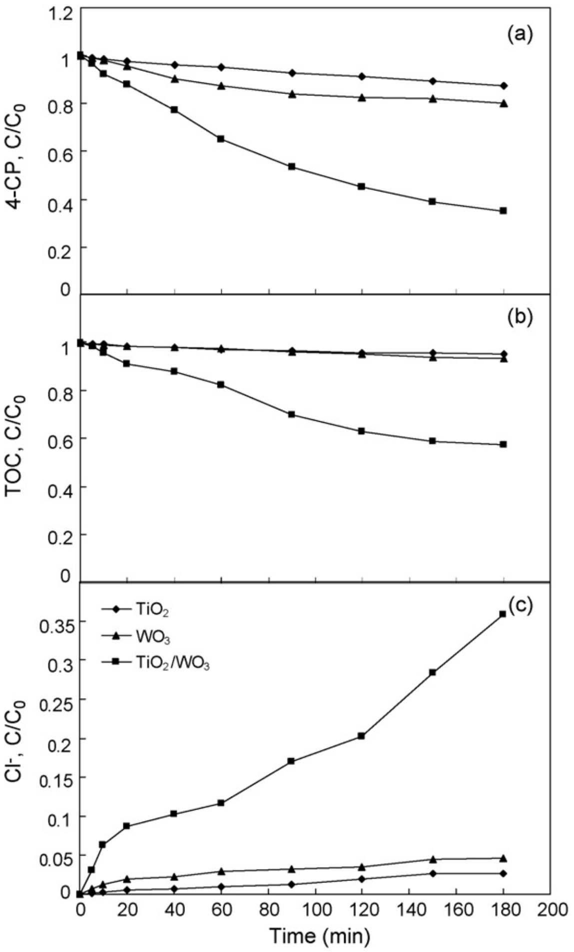

Fig. 4. Photodegradation of 4-CP at pH 7 in TiO_2, WO_3 and TiO_2/WO_3 systems at 435 nm, 4-CP 2×10^{-4} M, catalyst 1.2 g/L, 50 W light, and $T = 25\,°C$. (a) 4-CP, (b) TOC, and (c) chloride.

3.2. TiO_2/WO_3 and single catalyst systems

3.2.1. 4-CP degradation at 435 nm

The plots of 4-CP degradation at pH 7 at wavelength 435 nm are shown in Fig. 4a, with the corresponding TOC and chloride released data shown in Fig. 4b and c, respectively. The results clearly indicate that the removal of 4-CP up to 65% could be attained at 180 min in the TiO_2/WO_3 system, whereas there was insignificantly reduction of 4-CP for either TiO_2 or WO_3 system. A much higher hydroxyl radical concentration is found for the TiO_2/WO_3 system (Fig. 5c). Fig. 4b data further indicate an accumulation of intermediates since TOC reduction was only 40% at 180 min with the corresponding theoretical chloride release of about 38%.

In theory, the energy from the visible 435 nm light can only excite WO_3 (band edge 450 nm; 2.76 eV) and irradiated electrons are then transferring to the non-illuminated TiO_2 (band edge 390 nm; 3.18 eV), while the photoholes remained on WO_3 [6] or transferred to TiO_2 [22]. This electron transfer phenomenon resulting in a better charge separation may explain the observed higher efficiency of TiO_2/WO_3 system. On the other hand, the potential recombination of electrons and holes without interparticle electron transfer in the WO_3 alone system results in its poor performance. Since energy from 435 nm could hardly excite TiO_2, its poor performance is expected. Literature is replete with a better photocatalytic performance in coupled systems, e.g., degradation of CH_3OH in an TiO_2/WO_3 bilayer system with artificial sunrays [26], degradation of phenol and pentachlorophenol in an CdS/TiO_2 system at 406 nm [6].

3.2.2. pH effect

The free hydroxyl radical concentration is highest for the TiO_2/WO_3 system at pH 4 (Fig. 5b). 4-CP degradation as a function of pH is shown in Fig. 6. Lower pH favors the 4-CP degradation. The negatively changed of 4-CP (with a pK_a of approximately 9.43) at pH 10 may explain the poor performance at pH 10. The pH_{zpc} (zero point charge) for TiO_2 and TiO_2/WO_3 are 6.8 [24] and 6.4 [27], respectively. Thus, at pH 4, positively charged TiO_2/WO_3 surface exists. Also, the irradiation time plays a significant factor in the overall 4-CP degradation. Since the 1st-order rate constants between data up to 180 min and those of 480 min do not vary too much, all subsequent experiments were terminated at $t = 180$ min. Table 2 summarizes all the observed 1st-order rate constants under various conditions.

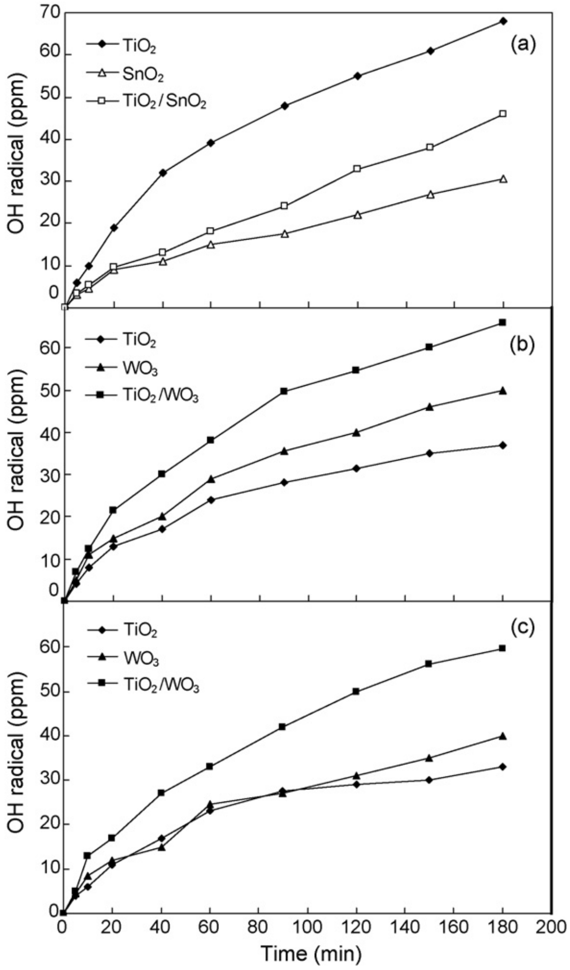

Fig. 5. Free hydroxyl radical concentrations (a) pH 4 at 369 nm, (b) pH 4 at 435 nm, and (c) pH 7 at 435 nm.

3.2.3. 4-CP degradation at 369 nm

The rationale for using 369 nm is that light energy could excite both TiO_2 and WO_3. In this way, it may lead to simultaneous electron transfer from TiO_2 to WO_3 and hole transfer from WO_3 to TiO_2 [6]. Thus, a better performance for the degradation of gaseous butyl acetate in the coupled TiO_2/WO_3 system at 350 nm [28], gaseous benzene and 2-propanol and liquid methyl blue [13], 1, 4-dichlorobenzene [16], gaseous 2-propanol [29] has been reported in the literature. Despite the enhanced performance with a better understanding of the increased surface acidity [13,28], highly UV photoindcued hydrophilic character of the TiO_2 surface in the presence of WO_3 [22], and direct proof of electron transfer from TiO_2 to c-WO_3 [14], the results of the present study are much different than those under 435 nm irradiation in that the coupled system performed poorly as compared to the single TiO_2 or WO_3 system (Fig. 7). In fact, the performance of TiO_2 alone is the best; after 180 min, only 20% 4-CP remained in the single TiO_2 system. For other pH results (pH 4 and 11), the trend is similar (data not shown). Others have also reported

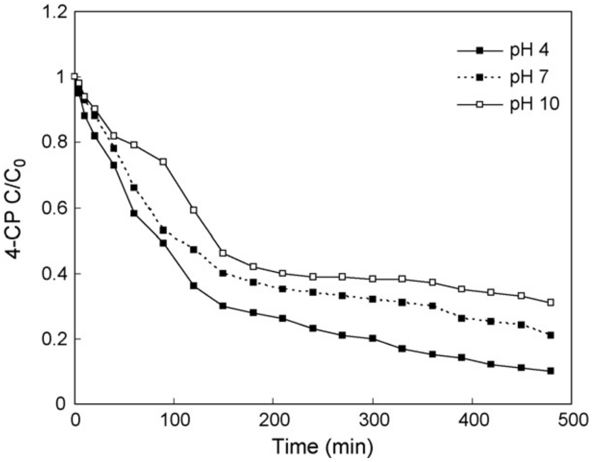

Fig. 6. Photodegradation of 4-CP as a function of pH in TiO_2/WO_3 system (light wavelength = 435 nm, 4-CP = 2×10^{-4} M, catalyst = 1.2 g/L, light power = 50 W and $T = 25\,°C$).

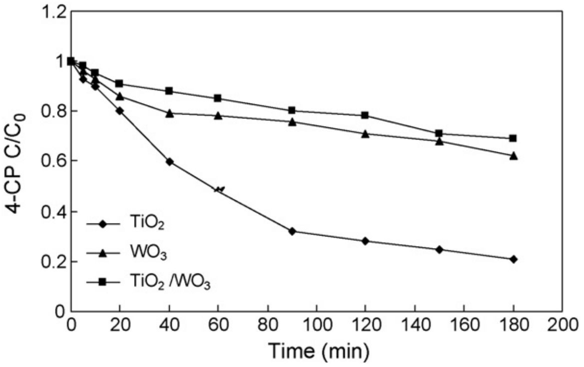

Fig. 7. Photodegradation of 4-CP at pH 7 in TiO_2, WO_3 and TiO_2/WO_3 systems (light wavelength = 369 nm, 4-CP = 2×10^{-4} M, catalyst = 1.2 g/L, light power = 50 W, and $T = 25\,°C$).

Table 2
Photodegradation rate constant (k, h^{-1}) in various systems

Semiconductor	Wavelength (nm)					
	369			435		
	pH 4	pH 7	pH 10	pH 4	pH 7	pH 10
TiO_2	1.068 (0.944)	0.708 (0.977)	0.504 (0.951)	0.078 (0.954)	0.003 (0.958)	0.042 (0.707)
SnO_2	0.060 (0.789)	0.090 (0.923)	0.204 (0.972)	0.036 (0.883)	0.003 (0.922)	0.042 (0.989)
TiO_2/SnO_2	0.204 (0.955)	0.306 (0.989)	0.366 (0.985)	0.120 (0.858)	0.003 (0.978)	0.060 (0.972)
WO_3	0.222 (0.978)	0.378 (0.970)	0.102 (0.986)	0.096 (0.977)	0.108 (0.948)	0.078 (0.953)
TiO_2/WO_3	0.180 (0.983)	0.132 (0.950)	0.108 (0.963)	0.504 (0.997)	0.378 (0.989)	0.288 (0.981)

The values in parenthesis are R^2.

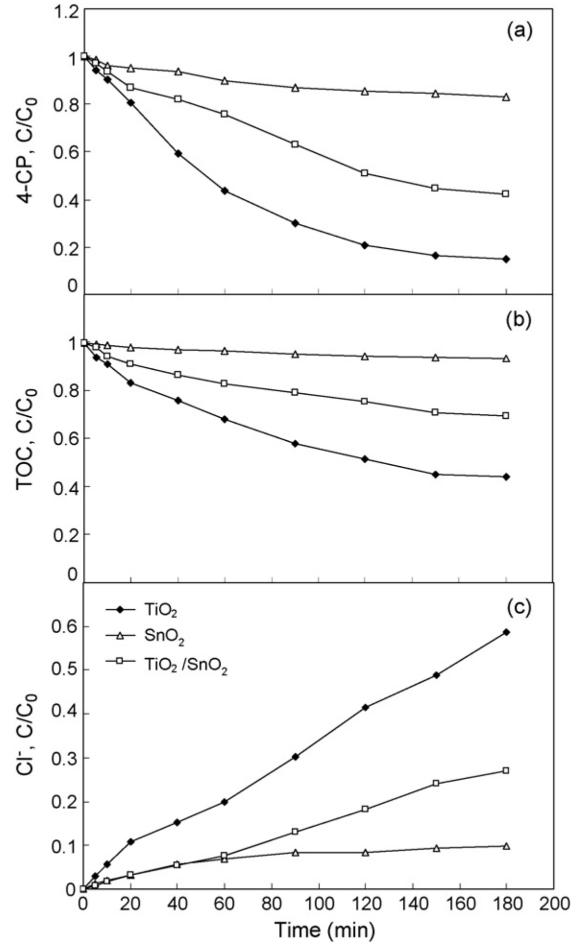

Fig. 8. Photodegradation of 4-CP at pH 7 in TiO_2, SnO_2 and TiO_2/SnO_2 systems at 369 nm, 4-CP 2×10^{-4} M, catalyst 1.2 g/L, 50 W light, and $T = 25\,°C$. (a) 4-CP, (b) TOC, and (c) chloride.

a poor photoactivity of the coupled TiO_2/WO_3 system for phenol degradation at pH 3 and 355 nm [6] and gaseous oxidation of CH_3CHO and liquid-phase degradation of 2-naphthol [14]. Tada et al. [14] attributed the poor performance to the decrease in the rate of electron transfer from the semiconductors to O_2. Keller et al. [28] further discussed the adverse effect of a high load of TiO_2/WO_3 in that it could act as recombination centers for electron-hole pairs resulting in the reduced efficiency. Unfortunately, the exact reason(s) for the observed poor performance of TiO_2/WO_3 is unclear.

3.3. TiO_2/SnO_2 and single catalyst systems

3.3.1. 4-CP degradation at 369 nm

Fig. 8 shows the 4-CP and TOC removal as well as the corresponding chloride release at 369 nm. The addition of SnO_2 onto TiO_2 does not enhance the photooxidation of 4-CP; TiO_2 alone is the best with 85% 4-CP removal and SnO_2 alone only removes about 20% 4-CP after 180 min. The hydroxyl radical concentrations follow the same trend, i.e., TiO_2 yields the highest concentration (Fig. 5a). Again, there is a significant accumulation of intermediates (Fig. 8b). In the presence of SnO_2, the hydrophilicity of the coupled TiO_2/SnO_2 system increases [30]; this characteristic should not inhibit 4-CP degradation. Literature indicates, however, a better performance of the coupled TiO_2/SnO_2 systems, e.g., dehydrogenation of methanol at 320–400 nm [8]. Despite the electron transfer from TiO_2 (390 nm; 3.18 eV) to SnO_2 (335 nm), Pilkenton and Raftery [23] reported that SiO_2/TiO_2 or TiO_2/SnO_2 film was less active in photodegradation of ethanol than a single TiO_2 system. They attributed the buildup of intermediates on the catalysts surface. Serpone et al. [6] also reported no improved phenol degradation for TiO_2/SnO_2 as compared to TiO_2 at 355 nm. The lower efficiency observed in the preset study may be due to the amount of SnO_2 incorporated into TiO_2, since its quantity influences the photoactivity [9]. As for 4-CP degradation at 435 nm, the poor performance (Fig. 9) is expected since the visible light cannot excite TiO_2 nor SnO_2. The TiO_2/SnO_2 system only slightly improved the 4-CP degradation, if any.

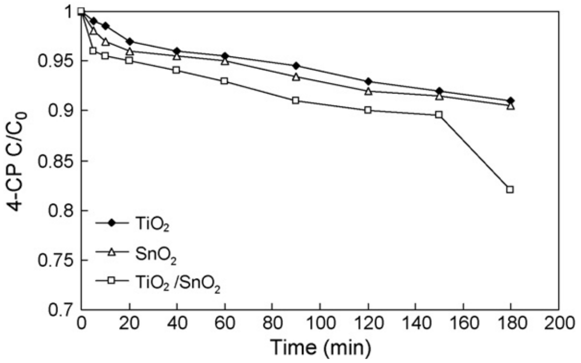

Fig. 9. Photodegradation of 4-CP at pH 7 in TiO_2, SnO_2 and TiO_2/SnO_2 systems (light wavelength = 435 nm, 4-CP = 2×10^{-4} M, catalyst = 1.2 g/L, light power = 50 W and $T = 25\,°C$).

4. Conclusion

To enhance 4-CP degradation rate and using the visible light energy source, the present study used two coupled systems, TiO_2/WO_3 and TiO_2/SnO_2. The important findings of this study were presented below.

1. The band edge wavelength increased to 475 nm, gap energy decreased to 2.61 eV and the specific surfaces area reduced to 37 m^2/g in the TiO_2/WO_3 system as compare to the single TiO_2.
2. In the TiO_2/WO_3 system, the degradation efficiency significantly increased as compared to single TiO_2 or WO_3 system at 435 nm wavelength. However, the TiO_2/WO_3 degradation of 4-CP at 369 nm was in fact inhibited.
3. In TiO_2/SnO_2 system, the degradation efficiency also suffered at 369 nm, and only slightly increased at 435 nm as compared to single TiO_2 or SnO_2 system.

Acknowledgement

The authors would like to thank the National Science Council of the Republic of China for financially supporting this research under Contract No. NSC 92-2211-E-002-007.

References

[1] A. Ikeda, C. Abe, T. Torimoto, B. Ohtani, Photochemical hydrogen evolution from aqueous triethanolamine solutions sensitized by binaphthol-modified titanium(IV) oxide under visible-light irradiation, J. Photochem. Photobiol. A: Chem. 160 (2003) 61–67.

[2] V. Iliev, D. Tomova, L. Bilyarska, L. Prahov, L. Petrov, Phthalocyanine modified TiO_2 or WO_3-catalysts for photooxidation of sulfide and thiosulfate ions upon irradiation with visible light, J. Photochem. Photobiol. A: Chem. 159 (2003) 281–287.

[3] K. Gurunathan, Photocatalytic hydrogen production using transition metal ions-doped gamma-Bi_2O_3 semiconductor particles, Int. J. Hydrogen Energy 29 (2004) 933–940.

[4] T. Ohno, T. Mitsui, M. Matsumura, Photocatalytic activity of S-doped TiO_2 photocatalyst under visible light, Chem. Lett. 32 (2003) 364–365.

[5] N. Serpone, E. Borgarello, M. Gratzel, Visible-light induced generation of hydrogen from H_2S in mixed semiconductor dispersions—improved efficiency through inter-particle electron-transfer, J. Chem. Soc. Chem. Commun. 6 (1984) 342–344.

[6] N. Serpone, P. Maruthamuthu, P. Pichat, E. Pelizzetti, H. Hidaka, Exploiting the interparticle electron-transfer process in the photocatalyzed oxidation of phenol, 2-chlorophenol and pentachlorophenol—chemical evidence for electron and hole transfer between coupled semiconductors, J. Photochem. Photobiol. A: Chem. 85 (1995) 247–255.

[7] R.A. Doong, C.H. Chen, R.A. Maithreepala, S.M. Chang, The influence of pH and cadmium sulfide on the photocatalytic degradation of 2-chlorophenol in titanium dioxide suspensions, Water Res. 35 (2001) 2873–2880.

[8] T. Kawahara, Y. Konishi, H. Tada, N. Tohge, S. Ito, Patterned TiO_2/SnO_2 bilayer type photocatalyst. 2. Efficient dehydrogenation of methanol, Langmuir 17 (2001) 7442–7445.

[9] Q.J. Liu, X.K. Yang, Q. Liu, B.L. Wang, X.H. Wu, Super-hydrophilicity of TiO_2/SnO_2 composite film, J. Inorg. Mater. 18 (2003) 1331–1336.

[10] J. Shang, W.Q. Yao, Y.F. Zhu, N.Z. Wu, Structure and photocatalytic performances of glass/SnO_2/TiO_2 interface composite film, Appl. Catal. A: Gen. 257 (2004) 25–32.

[11] H. Tada, Y. Konishi, A. Kokubu, S. Ito, Patterned TiO_2/SnO_2 bilayer type photocatalyst. 3. Preferential deposition of Pt particles on the SnO_2 underlayer and its effect on photocatalytic activity, Langmuir 20 (2004) 3816–3819.

[12] R. Suarez-Parra, I. Hernandez-Perez, M.E. Rincon, S. Lopez-Ayala, M.C. Roldan-Ahumada, Visible light-induced degradation of blue textile azo dye on TiO_2/CdO-ZnO coupled nanoporous films, Solar Energy Mater. Solar Cells 76 (2003) 189–199.

[13] Y.T. Kwon, K.Y. Song, W.I. Lee, G.J. Choi, Y.R. Do, Photocatalytic behavior of WO_3-loaded TiO_2 in an oxidation process, J. Catal. 191 (2000) 192–199.

[14] H. Tada, A. Kokrubu, M. Iwasaki, S. Ito, Deactivation of TiO_2 photocatalyst by coupling with WO_3 and the electrochemically assisted high photocatalytic activity of WO_3, Langmuir 20 (2004) 4665–4670.

[15] H. Lin, H. Kozuka, T. Yoko, Low-temperature crystallization of TiO2 films on arranged mono-layers by sol–gel method, Mol. Cryst. Liq. Cryst. 337 (1999) 217–220.

[16] Y.R. Do, W. Lee, K. Dwight, A. Wold, The effect of WO_3 on the photocatalytic activity of TiO_2, J. Solid State Chem. 108 (1994) 198–201.

[17] J.F. Jen, M.F. Leu, T.C. Yang, Determination of hydroxyl radicals in an advanced oxidation process with salicylic acid trapping and liquid chromatograph, J. Chromatogr. A 796 (1998) 283–288.

[18] C.H. Wu, Comparison of azo dye decolorization efficiency using UV/single semiconductor and UV/coupled semiconductor systems, Chemosphere 57 (2004) 601–608.

[19] C.H. Wu, G.P. Chang-Chien, W.S. Lee, Photodegradation of polychlorinated dibenzo-p-dioxins: comparison of photocatalysts, J. Hazard. Mater. 114 (2004) 191–197.

[20] C. Malagu, M.C. Carotta, E. Comini, G. Faglia, A. Giberti, V. Guidi, T.G.G. Maffeis, G. Martinelli, G. Sberveglieri, S.P. Wilks, Photo-induced unpinning of Fermi level in WO_3, Sensors 5 (2005) 594–603.

[21] F. Sanchez, T. Lopez, Effect of the preparation method on the band gap of titania and platinum-titania sol–gel materials, Mater. Lett. 25 (1995) 271–275.

[22] M. Miyauchi, A. Nakajima, T. Watanabe, K. Hashimoto, Photoinduced hydrophilic conversion of TiO_2/WO_3 layered thin films, Chem. Mater. 14 (2002) 4714–4720.

[23] S. Pilkenton, D. Raftery, Solid-state NMR studies of the adsorption and photooxidation of ethanol on mixed TiO_2–SnO_2 photocatalysts, Solid State Nucl. Magn. Reson. 24 (2003) 236–253.

[24] S. Sakthivel, B. Neppolian, M.V. Shankar, B. Arabindoo, M. Palanichamy, V. Murugesan, Solar photocatalytic degradation of azo dye: comparison of photocatalytic efficiency of ZnO and TiO_2, Solar Energy Mater. Solar Cells 77 (2003) 65–82.

[25] P. Peng, Y.Q. Ren, Preparation of non-TiO_2-SnO_2 composite film and its photocatalytic activity for toluene degradation, Chin. J. Catal. 24 (2003) 243–247.

[26] T. Takahashi, H. Nakabayashi, N. Yamada, J. Tanabe, Photocatalytic properties of TiO_2/WO_3 bilayers deposited by reactive sputtering, J. Vacuum Sci. Technol. A 21 (2003) 1409–1413.

[27] X.Z. Li, F.B. Li, C.L. Yang, W.K. Ge, Photocatalytic activity of WOx-TiO_2 under visible light irradiation, J. Photochem. Photobiol. A: Chem. 141 (2001) 209–217.

[28] V. Keller, P. Bernhardt, F. Garin, Photocatalytic oxidation of butyl acetate in vapor phase on TiO_2, Pt/TiO_2 and WO_3/TiO_2 catalysts, J. Catal. 215 (2003) 128–138.

[29] K.Y. Song, M.K. Park, Y.T. Kwon, H.W. Lee, W.J. Chung, W.I. Lee, Preparation of transparent particulate MoO_3/TiO_2 and WO_3/TiO_2 films and their photocatalytic properties, Chem. Mater. 13 (2001) 2349–2355.

[30] Q.J. Liu, X.H. Wu, B.L. Wang, Q.A. Liu, Preparation and super-hydrophilic properties of TiO_2/SnO_2 composite thin films, Mater. Res. Bull. 37 (2002) 2255–2262.